

New insights on obtaining phytoplankton concentration and composition from in situ multispectral Chlorophyll fluorescence

Christopher W. Proctor¹ and Collin S. Roesler^{2*}

¹School of Marine Sciences, University of Maine, Orono, Maine

²Ira C. Darling Marine Center and School of Marine Sciences, University of Maine, Walpole, Maine

Abstract

A three-channel excitation (435 nm, 470 nm, and 532 nm) Chlorophyll fluorometer (695 nm emission) was calibrated and characterized to improve uncertainty in estimated in situ Chlorophyll concentrations. Protocols for reducing sensor-related uncertainties as well as environmental-related uncertainties were developed. Sensor calibrations were performed with thirteen monospecific cultures in the laboratory, grown under limiting and saturating irradiance, and sampled at different growth phases. Resulting uncertainties in the calibration slope induced by natural variations in the in vivo fluorescence per extracted Chlorophyll yield were quantified. Signal variations associated with the sensors (i.e., dark current configurations, drift, and stability) and the environment (i.e., temperature dependent dark currents and contamination by colored dissolved organic matter [CDOM] fluorescence) yielded errors in estimating in situ Chlorophyll concentration exceeding 100%. Calibration protocols and concurrent observations of in situ temperature and CDOM fluorescence eliminate these uncertainties. Depending upon excitation channel, biomass calibration slopes varied between 6- and 10-fold between species and as a function of growth irradiance or growth phase. The largest source of slope variability was due to variations in accessory pigmentation, and thus the variance could be reduced among pigment-based taxonomic lines. Fluorescence ratios were statistically distinct among the pigment-based taxonomic groups, providing not only a means for approximating bulk taxonomic composition, but also for selecting the appropriate calibration slope to statistically improve the accuracy of in situ Chlorophyll concentration estimates. Application to 5 months of deployment in China Lake, Maine, USA reduced the error in estimating extracted Chlorophyll concentration from > 30% to < 6%.

Fundamental questions in aquatic ecosystems start with phytoplankton because of their role in structuring ecosystems and in the global carbon cycle. Although carbon is generally the currency of interest, separating phytoplankton carbon from total particulate organic carbon is not generally feasible. For this reason, phytoplankton biomass is typically described by the concentration of the Chlorophyll *a* (Chl *a*) pigment, which plays a

fundamental role in photosynthesis and is both unique to and ubiquitous in phytoplankton. The Chl *a* molecule is optically interesting in that it has two distinct absorption peaks that bracket the visible spectrum, each of which has shorter wavelength harmonics. The molecule also fluoresces. Thus, Chl concentration can be quantified in vitro by its absorption coefficient (UNESCO 1966; Strickland and Parsons 1968), and then, via a calibrated fluorometer, by its fluorescence intensity (Holm-Hansen et al. 1965; Lorenzen 1966). In vivo or in situ Chl *a* concentration has been estimated from in situ calibrated fluorometers for over 40 y (Lorenzen 1966) and much of our understanding about phytoplankton in their environment comes from fluorometric observations (e.g., Cullen 1982). And while the relationship between fluorescence and extracted Chl concentration does vary (Marra and Langdon 1993; Marra 1997), robust up-to-date laboratory calibration coupled with in situ vicarious calibration reduces the variability, yielding decades of observations of phytoplankton distributions in natural systems, measured on time and space scales relevant to physiological and physical processes (Dickey 1991).

*Corresponding author is now at Department of Earth and Oceanographic Science, Bowdoin College, Brunswick, ME 04011

Acknowledgments

The authors wish to thank John Peckenhams (George Mitchell Center for Environmental and Watershed Research, University of Maine) for use of the sensors and for support for CWP, under Environmental Protection Agency grant number CR-83293701-0. Doug Hankins (Western Environmental Technology Laboratory) was responsible for taking an idea and making it a sensor. CSR gratefully acknowledges support from the Office of Naval Research Environmental Optics and NASA Ocean Biology and Biogeochemistry programs.

DOI 10.4319/lom.2010.8.695

Recent advances in both sensors and platforms have broadened the capability for such observations, and yet there is still significant uncertainty in quantifying extracted Chl concentrations from in vivo fluorescence. The sources of variability include sensor design (sensitivity, response, kinetics, excitation, and emission wavebands; Neale et al. 1989); energy absorption and distribution in the cell; pigment packaging and pigment composition. Variability is observed as a function of species composition, relative pigment composition, cell size, nutrient status, growth phase, photoacclimation, and incident irradiance to name a few. Thus without ancillary information, the estimation of Chl concentration from in situ fluorescence, which would include contributions from phaeophytin as well (Cullen 1982; Marra and Langdon 1993), is within a factor of two at best and can be upwards of a factor of ten.

In this article, we report on a multispectral approach to eliminate or reduce the sources of uncertainty, yielding Chl concentration estimates with < 10% uncertainty, and additionally provide estimates of phytoplankton community composition as defined by pigment-based taxonomy.

Materials and procedures

The BBFL2 and 3X1M are two types of in situ optical sensors in the ECO Triplet class (WET Labs) that consist of multiple excitation and/or emission pairs. Each sensor has three light emitting diodes (LED) that provide excitation energy in a narrow waveband, and photodiode detectors to measure either the fluorescence or backscattering signal. The excitation beam enters the water at approximately 55°-60° from the optical head and the fluoresced light is received at an acceptance angle of approximately 140° (for backscattering the centroid angle is about 120°). An interference filter is used to reject scattered excitation light (or in the case of backscattering, fluoresced light; WETLabs ECO Users Guide). The ECO BBFL2 used in this study has three paired emitters and detectors to measure backscattering (660 nm), chromophoric, or colored dissolved organic matter fluorescence (CDOM; excitation at 370 nm, emission at 460 nm) and phycoerythrin fluorescence (PE, a pigment found in some cyanobacteria and cryptomonads; excitation at 540 nm, emission at 570 nm). The ECO 3X1M fluorometer was custom-designed to quantify the concentration and composition of light-harvesting algal pigments. It measures Chl fluorescence at 695 nm resulting from three excitation LEDs at 435 nm, 470 nm, and 532 nm. Excitation wavelengths were selected to provide isolation of the in vivo Chl *a* fluorescence intensity resulting from direct Chl *a* excitation (435 nm) and from energy transfer from the accessory Chlorophylls, carotenoids, and phycobilipigments. The exact selection of the LEDs was, in part, dependent upon industry standards (e.g., availability, standardization, power).

ECO Triplet measurements in the lab were collected using WET Labs software; data were collected in a 30-s burst sampling mode at 1 Hz resolution. To avoid errors associated with

sensor warm-up, the initial 5 s of data were discarded. The median and standard deviation from each of these “burst” samples were calculated. Systematic sensor responses were determined, including dark current readings (instrumental blank), environmental blanks (Cullen and Davis 2003), temperature dependence, and calibration with dilution series of monospecific cultures. The sensors were then deployed in natural waters to investigate the capabilities for determining algal biomass and composition in situ.

The general approach for determining a calibration is to perform a standard curve (i.e., measure the response to a dilution series of the calibrating constituent). The linear regression would be of the form:

$$Y = MX + B \quad (1)$$

where Y is the measured fluorescence response in digital counts (DC) for digital sensors or volts (V) for analog sensors. From this point onward, we will refer to digital sensors with digital count units. M is the slope of the response (DC (mg m⁻³)⁻¹), X is the concentration of the calibrating compound (mg m⁻³), and B is the intercept of the relationship (DC). In the absence of a blank signal, the intercept would be the dark current offset, DC_{dark}, the signal measured by the sensor in the absence of media (generally measured by placing black electrical tape over the excitation and emission windows). M is the calibration coefficient or calibration response, so that the calibrated value of any sample can then be determined from

$$C [\text{mg m}^{-3}] = (\text{DC}_{\text{sample}} - \text{DC}_{\text{dark}}) / M \quad (2)$$

The exact determinations of DC_{dark} and M are not trivial, and care is necessary to remove unwanted signals from the observations to achieve accurate results in C. Treatment of the blank is considered in the *Background fluorescence characterization* section.

Sensor characterization—The BBFL2 was provided with factory calibrations; the 3X1M was custom ordered and did not have a factory calibration against which to compare to our calibrations. Although both instruments were provided with factory measured dark current readings, we compared methods to determine the dark offset and instrument drift, as well as environmental factors that can affect measured fluorescence, such as temperature and background fluorescence. We investigated species-specific responses by characterizing the calibrations for different phytoplankton species grown under a range of growth conditions.

Temperature characterization—The natural systems in which these sensors were deployed were freshwater lakes that undergo large variations in water temperature. The optical properties of water itself are temperature-dependent (e.g., Morel 1974; Pegau et al. 1997) and must be included in the calibration procedure. In addition, diode detectors are known to be temperature-dependent (Roesler and Boss 2008),

Table 1. List of phytoplankton species used in calibrations. A variety of freshwater (F) and marine (M) species were selected from major taxa. Pigments abbreviations are allo (alloxanthin), alloPC (allophycocyanin), diad (diadinoxanthin), fuc (fucoxanthin), lut (lutein), neo (neoxanthin), PC (phycocyanin), PE (phycoerithrin), per (peridinen), viol (violaxanthin), zea (zeaxanthin) 19but (19-butanoyloxyfucoxanthin), and 19hex (19-hexanoyloxyfucoxanthin). Clone number preceded by C (CCMP) or U (UTEX).

Class	Species	Water	Accessory pigments	~Size (μm)	Label
Bacillariophyceae	<i>Asterionellopsis glacialis</i>	F	Chl <i>c</i> , fuc, diad	8-10 \times 28-44	C 139
Bacillariophyceae	<i>Chaetoceros gracilis</i> *	M	Chl <i>c</i> , fuc, diad	4-8 \times 4-10	C1318
Bacillariophyceae	<i>Thalassiosira pseudonana</i>	M	Chl <i>c</i> , fuc, diad	4-5 \times 4-6	C1335
Chrysophyceae	<i>Chromulina nebulosa</i>	F	Chl <i>c</i> , fuc, diad	5-6 \times 6-8	C 264
Cryptophyceae	<i>Cryptomonas reflexa</i>	F	Chl <i>c</i> , fuc, diad	16-20 \times 16-24	C 152
Cryptophyceae	<i>Rhodomonas</i> sp.	M	Chl <i>c</i> , allo, PE, PC	5-8 \times 6-14	C 758
Dinophyceae	<i>Amphidinium carterae</i> *	M	Chl <i>c</i> , per, diad	9-13 \times 12-18	C1314
Prymnesiophyceae	<i>Isochrysis galbana</i>	M	Chl <i>c</i> , fuc, diad, 19hex, 19but	9-13 \times 12-18	C1323
Chlorophyceae	<i>Ankistrodesmus falcatus</i> *	F	Chl <i>b</i> , vio, lut, neo	1-3 \times 35-65	U 749
Chlorophyceae	<i>Dunaliella tertiolecta</i> *	N	Chl <i>b</i> , vio, lut, neo	5-6 \times 6-7	C 364
Cyanophyceae	<i>Anabaena</i> sp.	F	zea, PC, alloPC,	filamentous	C2066
Cyanophyceae	<i>Synechococcus</i> cf <i>bacillus</i>	M	zea, PC, alloPC, PE	2 \times 4-8	C1261
Cyanophyceae	<i>Synechococcus</i> sp.	M	zea, PC, alloPC, PE	1 \times 1-3	C1334

*Indicates species used in growth experiments.

although temperature compensation is a recent improvement. Temperature calibrations were performed on all sensors. The optical faces were coated with a layer of black electrical tape, and measurements were taken in a non-reflective black bucket filled with filtered Milli-Q water. A Neslab/Endocal RTE-100 unit controlled the temperature over the range 1-30°C at 5°C increments. A Hanna digital thermometer was used to verify the water temperature with 0.1°C resolution. The instruments were submerged and allowed to equilibrate at each temperature for 3 min to replicate thermal equilibrium.

Background fluorescence characterization—Inland and coastal waters often contain very high concentrations of CDOM that was thought to impact Chl retrieval (Roesler et al. 2006). CDOM has strong fluorophores (e.g., Coble 2007) that may impact the retrieval of pigment fluorescence by absorbing the excitation energy, absorbing the emission energy, and/or contributing fluoresced energy to the detector (i.e., through spectral leakage or the fluorescence tail). Freshwater samples were collected from four environmentally distinct locations in Maine: China Lake (a large, colored lake), Pickerel Pond (a small, clear pond), Sunkhaze Stream (which flows through Sunkhaze bog and contains very high concentrations of CDOM), and the Piscataquis River (which contains high amounts of agricultural runoff). Samples were filtered through glass fiber filters (Whatmann GF/E, nominal pore size 0.7 μm) to remove particulates (note that this filter was selected to obtain closure with the particles captured on the filter for Chl analysis). Sensor response was characterized for a 1:2 stepwise dilution of each sample over a 6-fold range over the detection range for each instrument. Observations were taken in both a 12-L nonreflective black bucket and a 1-L glass beaker to investigate potential effects due to differences in optical and physical path length. Milli-Q water was used as the reference mate-

rial and as the diluent. Filtrate absorption was measured with a Cary 3E UV-Vis Spectrophotometer in 1-cm cuvettes in dual beam mode over the spectral range 250 nm to 900 nm (Bricaud et al. 1986; Roesler et al. 1989; Belzile et al. 2006), referenced to Milli-Q water.

Algal pigment calibrations—The Chl *a* calibration factors for the 3X1M and the BBFL2 PE fluorometers were quantified using 13 monospecific fresh and marine algal cultures grown under a range of conditions (Table 1). Each culture was grown under high and low growth irradiance and four of the cultures (*C. gracilis*, *A. carterae*, *D. tertiolecta*, and *A. falcatus*) were also used to investigate the variation in calibration factors resulting from growth phase.

Phytoplankton cultures were obtained from the Provasoli-Guillard National Center for Culture of Marine Phytoplankton (CCMP, Boothbay Harbor, USA) and University of Texas Culture Collection of Algae (UTEX, Austin, USA). Thirteen species of freshwater and marine phytoplankton were selected to encompass major pigment-based taxonomic groups, a range of cell sizes, and representative species common to freshwater environments in Maine. Batch cultures were maintained at 20°C and grown under a 12:12 days-night cycle illuminated by cool white fluorescent bulbs. Irradiance was measured using a LICOR quantum sensor. Each species was grown at two irradiances, 50 and 270 $\mu\text{mol photon m}^{-2}\text{s}^{-1}$ for eukaryotes and 10 and 50 $\mu\text{mol photon m}^{-2}\text{s}^{-1}$ for the cyanobacteria, henceforth referred to as “low” and “high” growth irradiance (L and H, respectively). Freshwater species were grown in DY-V media and marine species were grown in f/2 media obtained from CCMP (Andersen 2005). Cultures were acclimated to their growth irradiances in a semi-continuous batch mode for more than ten generations. Growth rates were determined from observations of in vivo fluorescence measured at the same

time each day with a Turner 10-AU bench top fluorometer (Andersen 2005). Triplicate cultures were inoculated into 50 mL test tubes allowed to reach exponential phase and then inoculated into 1-L glass flasks and harvested in exponential phase. This step-up in volume was used to minimize stress on the cultures, maintain balanced growth responses, and yield sufficient volume. The full dynamic range of the 3X1M was not tested because although it is capable of reading over 4000 DC, that would require phytoplankton concentrations of greater than 100 mg Chl m^{-3} , a concentration atypical of exponential growth phase and rare in natural environments (except in extreme cases). Typical harvesting concentrations ranged from 30 mg Chl m^{-3} to 60 mg Chl m^{-3} and 2500 DC to 3500 DC.

Dilution calibrations—Two 3X1M triplet sensors were calibrated by quantifying the fluorescence response in the set of monospecific cultures grown in batch under controlled high (H) or low (L) light conditions. Fluorescence response was measured over a two order of magnitude dilution series (approximately 0.5 to 50 mg Chl m^{-3} in six to eight dilutions). This number was experiment-specific and depended on how many 1:2 dilutions were needed to reach the sensor's sensitivity threshold. Triplet readings were performed in a 1-L glass beaker set on a black cloth in a dim room. Cultures were given half an hour to adapt to the room's light after being removed from the growth chamber, to avoid the effects of rapid photosystem changes such as the xanthophyll cycle (Lutz et al. 2001). Dilutions were performed with Milli-Q water or 0.2 μ m filtered seawater, appropriate to the specific culture medium. BBFL2 measurements were taken for the first dilution of all cultures and on the full dilution series for the 3 species of cyanobacteria to calibrate the phycoerythrin channel.

Triplicate samples of each dilution were collected for fluorometric Chl analysis (Yentsch and Menzel 1963; Holm-Hansen et al. 1965). Phytoplankton absorption was determined spectrophotometrically (Cary 3e UV-VIS) over the wavelength range 250 nm to 900 nm using the quantitative filter technique (Mitchell 1990) as modified by Roesler (1998). Methanol extraction was used to remove the contribution by non-algal particles (Kishino et al. 1985). When samples could not be immediately analyzed, filters were stored in liquid nitrogen.

Growth calibrations—The effect of growth phase on the fluorescence to extracted Chl ratio was studied by comparing these dilution calibrations with measurements taken while the cultures were actively growing from inoculation to harvest phases. 3X1M fluorometer measurements were taken daily during the growth of the *A. carterae*, *C. gracilis*, and *D. tertiolecta* (H) and (L) cultures. The typical range in Chl concentration was 1 to 25 mg/m³ over a 6-d growth experiment. Duplicate samples were collected for fluorometric Chl analysis, and the volume removed was replaced with fresh media (and accounted for in the determination of growth rates).

In situ deployment—The WET Labs 3X1M and BBFL2 sensors were deployed in China Lake for nearly 5 months (four

deployments) to investigate natural variability in phytoplankton concentration and composition. China Lake serves as a domestic water source for the surrounding towns of China and Vassalboro. It has a surface area of approximately 16 km², with an average depth of 8.5 m and a maximum depth of 25.9 m. The lake is very colored and has a tendency for eutrophication (PEARL 2007).

The sensors were deployed 1 m below the surface, attached to an anchored stainless steel frame suspended by a buoy. Water depth was approximately 3.5 m. The sensors were aligned vertically facing downwards to avoid direct solar contamination. The sensors were controlled and powered by a WET Labs DH4 data handler and 2 ECO battery packs. Data were collected every 15 min for 15 s at a 1 Hz data rate. Ancillary analyses were performed on discrete water samples when the sensor was retrieved for maintenance and included triplicate extracted Chl concentration and spectrophotometric dissolved and particulate absorption. In between deployments, the data were downloaded, the sensor was cleaned, and pure water calibrations performed to track the drift in the instruments.

Assessment

Sensor variability

Dark counts. Dark current digital counts (DC_{dark}) were tracked to characterize sensor drift and to accurately subtract the instrumental offset from sample observations. Sensor electronics that measure digital counts read greater-than-zero even in the absence of fluorescing material, and this offset must be subtracted from DC_{sample} (Eq. 2). No unequivocal protocol for measuring DC_{dark} has been established, so we investigated readings resulting from a range of scenarios used by various laboratories: the optical face taped and untaped in air (aimed across a dimly lit room away from walls), Milli-Q water, and 0.2- μ m filtered seawater (FSW) from Boothbay Harbor, Maine. Over the 3-y study, the 3X1M and BBFL2 were found to be stable without a significant drift in the median readings; however there were significant differences between the methods of measuring the dark counts (Table 2). Dark counts were lowest and most consistent using the configurations of the following: taped in MQ, taped in FSW, and taped and untaped air readings. Untaped readings in air were higher than taped readings in water, regardless of water purity. Immersed untaped readings were always higher due to fluorescence in the diluent (see CDOM impacts below). Immersion of untaped sensors in Milli-Q yielded values 10% higher in the 435 nm channel, 14% higher in the 470 nm, and 15% in the 532 nm channels. Immersion of untaped sensors in filtered seawater yielded values 12% higher in digital counts than taped filtered seawater in the 435 nm excitation channel, approximately 34% higher in the 470 nm and 14% higher in the 532 nm.

Temperature impact on DC_{dark}. Media temperature increased the DC_{dark} digital counts of the 3X1M by approximately 0.45, 0.31, and 0.36 (DC (°C)⁻¹), respectively for the

Table 2. Digital count variations in dark current readings. Serial number SN001 shown for illustrative purposes, SN003 had comparable ranges. Values represent median and standard deviations of 30 seconds burst samples.

Configuration	435 nm	470 nm	532 nm
Taped air	230 ± 14	65 ± 2	68 ± 2
Untaped air	231 ± 12	66 ± 1	69 ± 1
Taped MilliQ	207 ± 15	65 ± 2	68 ± 3
Untaped MilliQ	227 ± 11	74 ± 3	78 ± 2
Taped FSW	210 ± 8	65 ± 1	69 ± 1
Open FSW	236 ± 15	87 ± 4	79 ± 3

FSW, filtered seawater.

435 nm, 470 nm, and 532 nm excitation channels. There was no temperature impact on DC_{dark} for the BBFL2 phycoerythrin sensor and the CDOM fluorometer below 25°C, but the impact was ~ 0.20 (DC ($^{\circ}C$) $^{-1}$) on the backscattering channel.

Temperature can have a significant effect on estimates of biomass. Our 3X1M biomass calibrations were done at approximately 24°C. Seasonally, the in situ temperatures can be nearly 25°C colder; consequently, if uncorrected the 3X1M would underestimate Chl by nearly ten counts for the 435 nm channel, which could lead to an underestimation of the in situ Chl concentration of up to 0.5 mg Chl m^{-3} . Although this difference in concentration may not be important during a bloom, it can be equivalent to the wintertime Chl value and thus yield a 100% error, likewise for cold waters with low standing stock such as temperate or polar ocean waters.

Comparing different versions of the 3X1M. To investigate differences between different serial numbers of the same instrument, two 3X1M sensors were used in characterization experiments. The 3X1M-001 (SN001) and 3X1M-003 (SN003) both demonstrated linear calibrations relating fluorescence to biomass. Both 3X1M sensor calibrations shared similarities in grouping of algal classes, and similar amounts of error due to differences in pigmentation and physiology. However, each sensor had unique calibrations due to differences in factory-determined gain settings. In particular, the 532 nm excitation channel in SN003 had a much lower dynamic range than the SN001. While the 3X1M-001 detected an approximate 5-fold range of fluorescence for typical cultures, the 3X1M-003 only detected a doubling. The ratios of the SN003/SN001 slopes were 1.44 ± 0.10 , 0.93 ± 0.07 , and 0.15 ± 0.03 for the three channels. These differences between sensors of the same model and their factory calibrations demonstrate the importance of performing robust calibrations for each sensor and not relying on “out of the box” factory calibrations.

Pigment variability

Absorption. Pigment absorption characteristics varied between and within phytoplankton taxonomic lineages, although the similarities of species within lineages were pronounced (Fig. 1). The spectral shape of the absorption coefficient

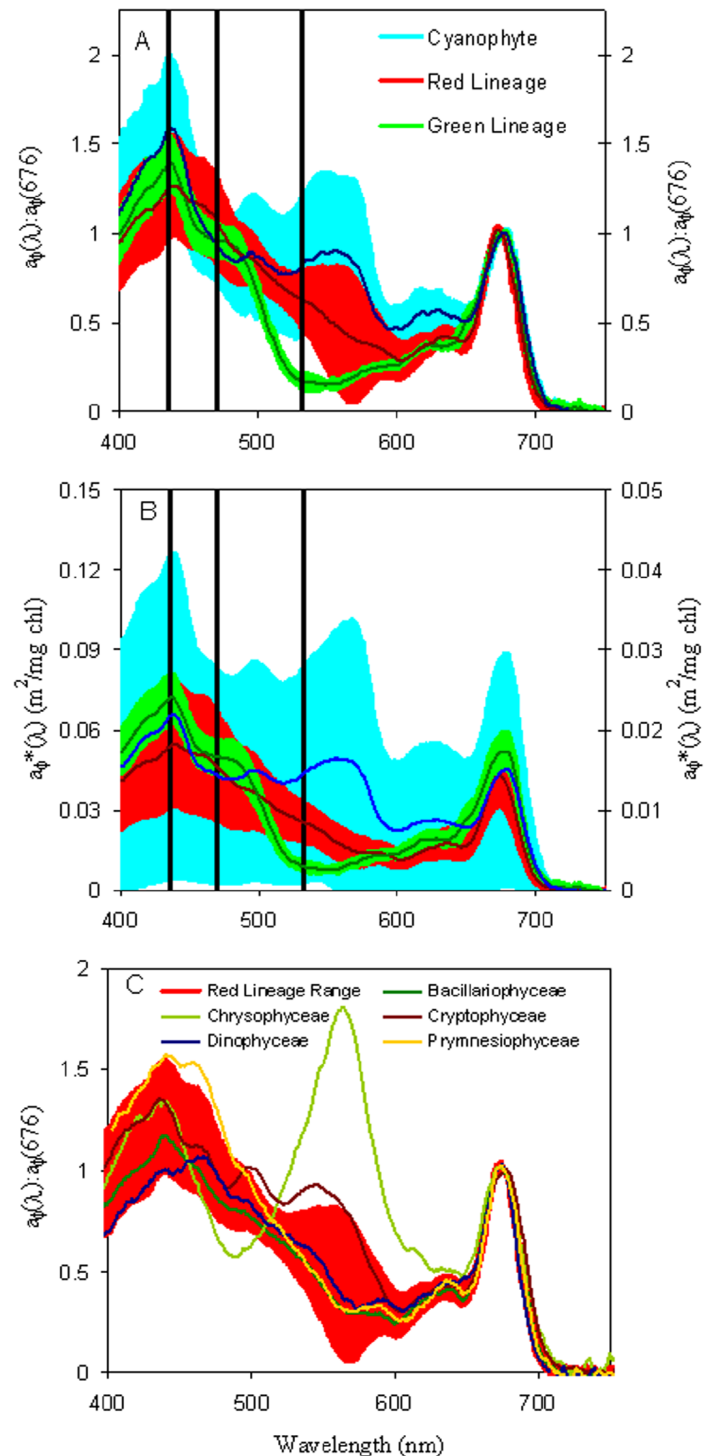


Fig. 1. Average absorption spectra of algal cultures in Table 1, separated by lineage (see text) and scaled by (A) Chl *a* red absorption peak at 676 nm or (B) Chl *a* concentration (Red and Green Lineage values are on the right hand scale). Vertical bars show the 3X1M excitation wavelengths in relation to pigment absorption peaks. Colored bands indicate absorption standard deviation for each lineage. (C) Median absorption spectra of diverse red lineage algal cultures scaled by the Chl *a* red absorption peak at 676 nm, shown with representative spectra for each of the classes in Table 1.

cients scaled to the Chl *a* red absorption peak at 676 nm (Fig. 1A) varied most in the waveband 500 nm to 600 nm, associated with the spectral band for carotenoid and phycobilipigment absorption. The Chl-specific absorption spectra (absorption scaled by extracted Chlorophyll concentration with units $m^2 mg^{-1}$) exhibited even larger variation due primarily to the high values and significant within group-variability exhibited by the Cyanophytes (Fig. 1B).

Changes in fluorescence due to changes in Chl concentration. Typical individual calibrations ranges spanned approximately a 6-fold range of digital counts and a 100-fold range of Chl concentration to characterize both the lower detection limit of the sensor ($\sim 0.5 mg Chl m^{-3}$) and the upper range of reasonable in situ Chl concentrations (i.e., $\sim 50 mg Chl m^{-3}$). For each of the dilution series calibration experiment, there was a linear relationship between extracted Chl and measured fluorescence (with $n = 6$ to 8 observations per experiment, r^2 values exceeded 0.97). This relationship was also observed in the growth experiment calibrations with the exception of *C. gracilis* (H; $r^2 > 0.86$), *D. tertiolecta* (L; $r^2 = 0.92, 0.89, 0.67$ for 435 nm, 470 nm, 532 nm, respectively) and *A. falcatius* (H; $r^2 > 0.92$ for 532 nm); standard error in the slope calculation was generally $< 10\%$). The 435 nm channel displayed the largest absolute range in fluorescence followed by the 470 nm, then the 532 nm channels. These differences are due in part to the optical characteristics of the phytoplankton (i.e., ranges in both absorption and fluorescence yield at each channel; Fig. 1) and in part due to sensor characteristics (in particular the different gain setting for each LED). There was a 6-fold increase from the minimum slope measured at the 435 nm channel to the maximum slope, and the range for the 470 and 532 nm channels was 10-fold and 40-fold, respectively (Fig. 2).

Variability between species. The Chl calibration response slopes were grouped taxonomically into phytoplankton of green lineage, red lineage, and cyanobacteria (Falkowski et al. 2004; Falkowski and Raven 2007, noting that these are evolutionary distinctions), with each pigment class sorted in ascending magnitude of slope (Fig. 2) for the 435 nm excitation channel. There was overlap in the response between groups but some patterns emerge within and between the pigment groups. The green lineage and red lineage phytoplankton had a similar range in response slopes in the 435 nm and 470 nm excitation channels. The cyanobacteria had much lower response slopes with the exception of the low light acclimated *Anabaena* sp., and the groups were very distinct at the 532 nm channel. Within each lineage grouping, phytoplankton of the same species had similar response slopes regardless of irradiance acclimation. The median slope values for all species, and each of the 3 taxonomic groupings was calculated (Table 3). Chlorophytes had the highest median slope for the 435 nm channel but the lowest for the 532 nm. Cyanobacteria had the lowest median slopes for the 435 and 470 nm channels, but the highest slope for the 532 nm. Differences in slope between a species grown at different light

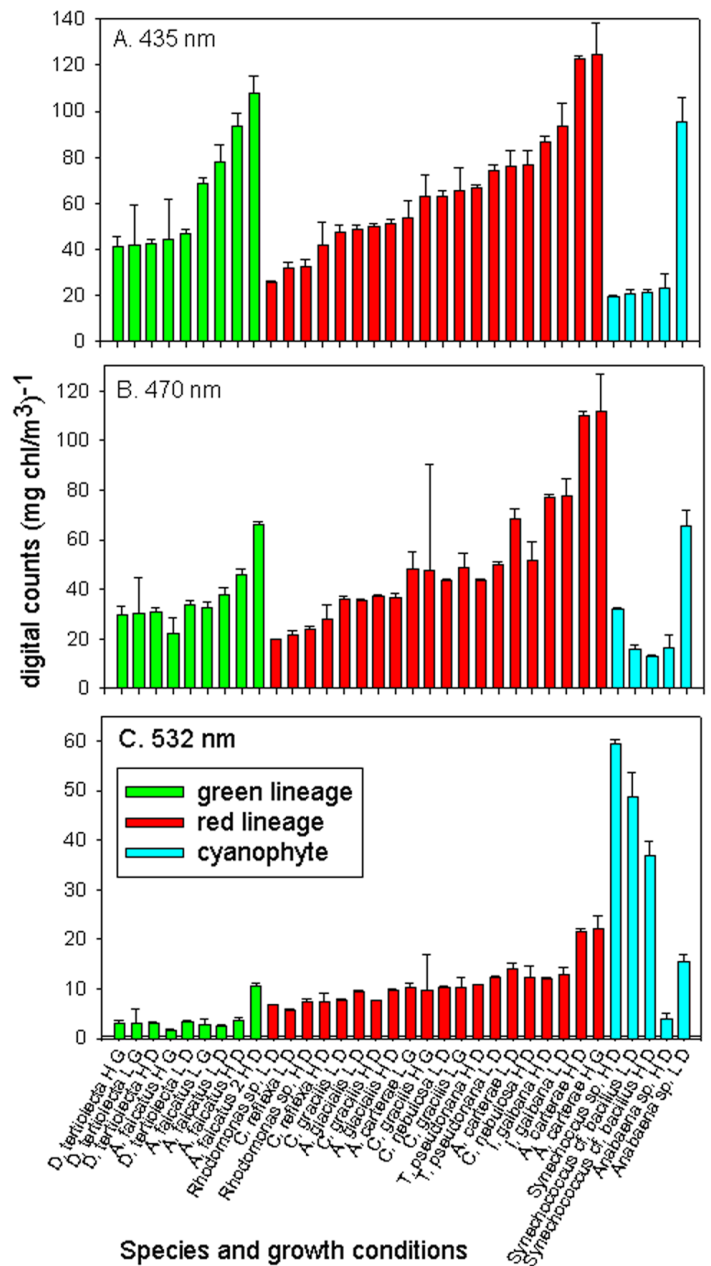


Fig. 2. Chl calibration slopes (DC [mg Chl m^{-3}] $^{-1}$) for the A. 435 nm, B. 470 nm, and C. 532 nm wavelength excitation channels. Species names are followed by culture growth conditions: acclimated growth irradiance (L or H) and growth or dilution experiment (G or D).

levels could be distinguished statistically, but growth irradiance impacted the slope approximately the same amount that growth phase did (13%, 13%, 2% versus 12%, 13%, 5% on average, for 440 nm, 470 nm and 532 nm), for all species excluding the cyanophytes. These ranges were certainly less than those observed between species. For the cyanophytes, the greater than order of magnitude range in slope in response to growth irradiance was due to *Anabaena* sp. In total, approx-

imately 71% of the percent difference between slopes was explained by species (pigment composition) differences, 12% explained by relative intracellular pigment concentrations (growth irradiance), and 17% by growth phase.

Pigment ratios. Absorption spectra scaled to the red absorption peak at 676 nm were averaged by pigment class (Fig. 1A.). Each pigment class has a unique spectral shape, dominated by its respective pigment complement. Superimposed on this figure are vertical bars showing the location of the 3X1M excitation channels. While all phytoplankton have strong absorption at 435 nm due to the Soret Chl absorption peak, the relative magnitude of that absorption to the other channels varies greatly. Green phytoplankton lack significant carotenoid concentrations thus have very low absorption at 532 nm whereas Cyanophytes have very strong absorption there due to phycobilipigments. The large variability observed within the red lineage is due to the phycobilipigment-containing groups (e.g., *Rhodomonas* sp.). Within each pigment class, a broad range in individual absorption spectra was observed associated with diverse pigment complements (Fig. 1C). Whereas there are a few species with exceptional pigmentation (e.g., the absorption spectra of Cryptophyceae and Cryptophyceae), there is a dominant spectral shape associated with pigmentation, particularly between the three excitation channels.

Fluorescence responses measured by the 3X1M and corrected for dark counts were used to compute the average fluorescence ratios for each culture. Error associated with individ-

Table 3. Summary of the Chl biomass calibration slopes for thirteen species, two growth irradiances, and growth phase for the 3X1M-001. Species were grouped into pigment-based evolutionary lines. Fluorescence response slopes were generated for each of the 3X1M excitation channels plus or minus the absolute value of the difference between the slope and its 95% confidence intervals. Slope units are digital counts of fluorescence divided by Chl concentration (e.g., DC [mg Chl m⁻³]⁻¹).

Pigment Class	Slope (DC [mg Chl m ⁻³] ⁻¹)		
	435 nm	470 nm	532 nm
Green lineage	47.01 ± 25.38	32.45 ± 12.84	3.09 ± 2.61
Red lineage	58.51 ± 27.16	43.74 ± 26.21	10.26 ± 4.36
Cyanophyte	21.34 ± 33.32	16.26 ± 22.07	36.73 ± 22.96
All cultures	51.58 ± 28.55	37.04 ± 23.90	9.49 ± 12.71

Table 4. Median ± standard deviation Chl fluorescence ratios measured by the 3X1M and grouped by pigment lineage. Dark current offsets were removed, and temperature and CDOM corrections were applied to each reading prior to ratio calculation.

Pigment class	Channel ratios		
	470 nm/532 nm	435 nm/470 nm	435 nm/532 nm
Green lineage	8.50 ± 0.74	1.48 ± 0.12	13.72 ± 1.30
Red lineage	4.51 ± 0.19	1.33 ± 0.06	5.95 ± 0.59
Cyanophyte	0.53 ± 0.34	1.40 ± 0.06	0.61 ± 0.40

ual ratios was less than 5%, except in green lineage cultures grown at high light. Each pigment lineage was statistically unique for the 435 nm/532 nm and 470 nm/532 nm ratios. Statistical uniqueness was determined with an ANOVA, post hoc Tukey's Significance Difference Test, $P < 0.05$. The medians for each pigment group ratio are given in Table 4. The 435 nm/470 nm ratio was the most similar for all species, with differences of 5% to 11% between pigment group medians. Fluorescence ratios for the 470 nm/532 nm and 435 nm/532 nm channels were very distinguishable between and within pigment lineages, particularly the 470 nm/532 nm. Cyanophytes had the lowest median ratios for these channels, the red lineage ratios were almost nine times higher, and the green lineage ratios were a factor of two greater than the red.

Differences in pigment ratios broken down by taxonomic class are shown in Fig. 3. Although it is difficult to discern statistically significant differences between taxonomic groups using the 435 nm/470 nm ratio, there are significant differences using the other two ratios. Cyanophyceae and Chlorophyceae stand out respectively at the low and high end of these ratio ranges. Within the red lineage, however, each class is statistically separable using the combination of the three excitation ratios.

Environmental variability

CDOM and environmental blank readings. Whereas the instrument background signal is removed via the dark reading, other fluorescence signatures arise in the environment that are not associated with Chl fluorescence. These signals constitute the environmental blank (Cullen and Davis 2003). These background signals can be quite large, particularly for waters rich in CDOM, which was found to "contaminate" the 695 nm emission detection resulting from all three of the 3X1M excitation channels (and subsequently has been found in Chl fluorometers from other manufacturers, as well, as it is not an instrumental problem but a natural signal). The intensity of the apparent Chl fluorescence emission by CDOM increases linearly with CDOM concentration (determined by both BBFL2-measured CDOM fluorescence and spectrophotometric CDOM absorption), and decreased with excitation wavelength (Fig. 4), consistent with an exponential decrease in the absorption of the excitation wavelength. The linear relationship between BBFL2 F_{CDOM} and 3X1M F_{Chl} was significant for each excitation (r^2 values of 0.99, 0.99, 0.97 respectively, $n = 19$). The water used in the CDOM calibration experiment came from four environmentally distinct locations

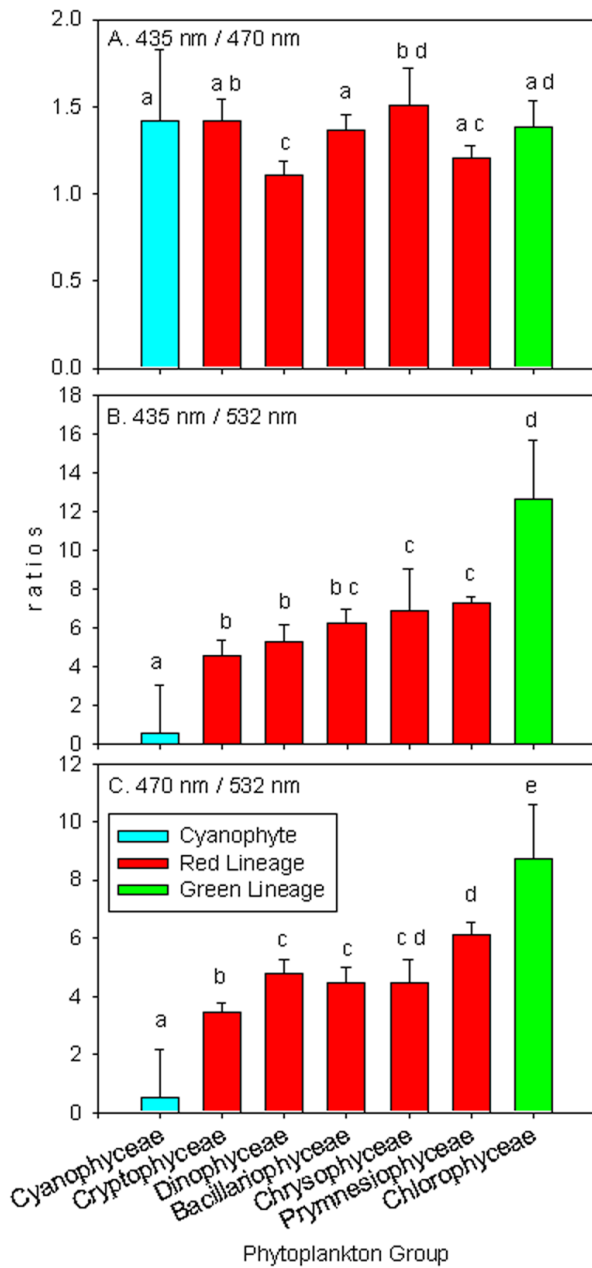


Fig. 3. Fluorescence ratios for phytoplankton classes measured with the 3X1M. Unshared letters over bars indicate statistically unique ratios (determined using an ANOVA; post hoc Tukey’s Significance Difference Test, $P < 0.05$). Bar coloration denotes phytoplankton pigment class: cyan for Cyanophyte, red for red lineage, and green for green lineage.

throughout the state of Maine. Although the CDOM in these waters had two distinct quantum yield relationships between absorption and BBFL2 CDOM fluorescence (Belzile et al. 2006; Roesler et al. 2006), there was a uniform relationship between the BBFL2 CDOM fluorometer and the fluorescence emission measured by the 3X1M. Therefore, the composition of the CDOM is not important for these corrections, just the fluorescence intensity.

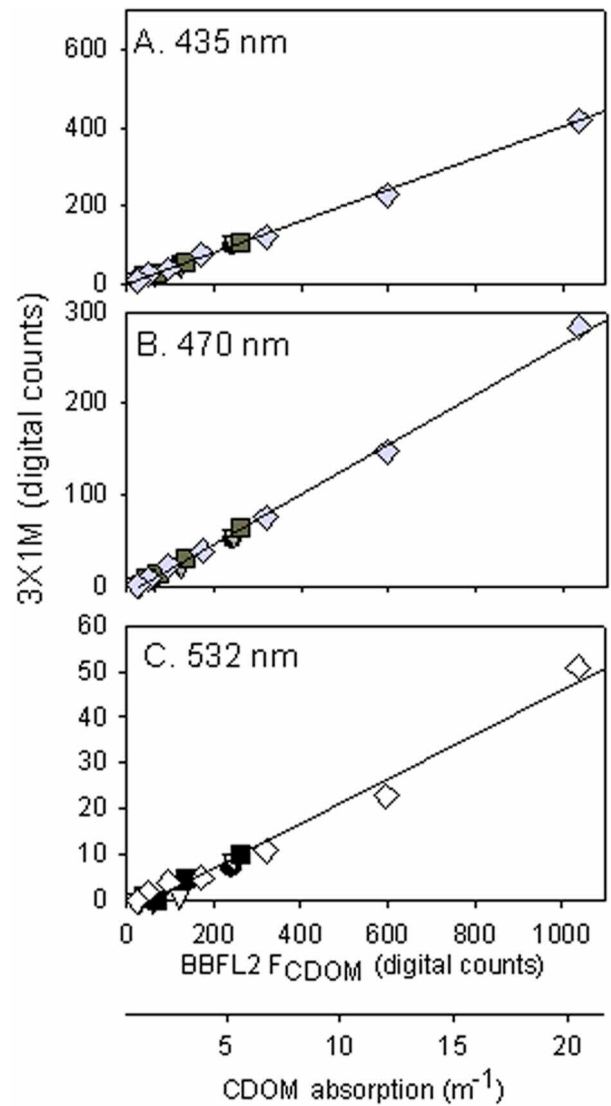


Fig. 4. Apparent Chl fluorescence resulting from A. 435 nm, B. 470 nm, and C. 532 nm LED excitation as a function of BBFL2-CDOM fluorescence measured in a nonreflective bucket and CDOM absorption coefficient at 370 nm for water collected from diverse locations in Maine, USA (China Lake, circle; Pickerel Pond, triangles; Piscataquis River, squares; Sunkhaze bog, diamonds).

CDOM fluorescence “contaminated” all three excitation channels, and although the effects decreased at longer wavelength excitations, due to exponentially decreasing absorption, they were significant for all channels. Correcting for CDOM is extremely important when interpreting in situ data, particularly if working in inland or coastal waters; otherwise Chl is likely to be overestimated (Roesler et al. 2006). For example, many digital fluorometers excite at 470 nm. Several natural samples collected through inland Maine waters and filtered to remove particles, yielded on the order 50 counts in the 3X1M 470 nm excitation channel (after dark corrections applied; undiluted readings in Fig. 4). This order of fluores-

Table 5. Range in environmental parameters for each deployment in China Lake, Maine, USA. a_{CDOM} is the absorption coefficient for colored dissolved organic matter at 370 nm, the excitation wavelength of the CDOM fluorometer in the BBFL2.

Deployment	Temperature (°C)	Chl (mg m ⁻³)	a_{CDOM} (m ⁻¹)
18 Aug 2006–29 Aug 2006	21.8-25.3	7.60-15.18	2.24-2.70
2 Sep 2006–25 Sep 2006	19.1-22.7	7.46-14.01	2.09-2.70
8 Oct 2006–5 Nov 2006	9.6-16.8	4.37- 7.75	2.09-3.26
17 May 2007–2 July 2007	11.2-24.0	2.62-13.83	1.22-2.65

cence counts, which is due to the contamination by CDOM fluorescence, will lead to an overestimation of Chl between 0.4-3.9 mg Chl m⁻³, depending upon the calibration slope applied. Typical Chl concentrations in inland waters are 5-20 mg Chl m⁻³, whereas coastal Chl concentrations often range from 1-5 mg Chl m⁻³. In the extreme case of the highly colored water from Sunhaze bog, 290 digital counts in the 3X1M 470 nm channel were due to the CDOM fluorescence. Depending on which calibration was used, Chl would be overestimated by 2.7-22.3 mg Chl m⁻³!

In situ application. The 3X1M and BBFL2 were deployed in China Lake over the course of three seasons over two calendar years to collect observations of the fall and spring phytoplankton growth seasons, respectively (Table 5). Daily median ratios of 3X1M fluorescence in the different channels were calculated (Fig. 5). These ratios were used to determine phytoplankton composition (Fig. 3) and the appropriate calibration slope for that pigment class (Fig. 2). The median calibrations for the cyanophyte and red lineage were averaged during the period between October and November where Fig. 5b suggests a mixed composition and Fig. 5A indicates there are cyanophytes present.

Changes in biomass were observed as 3X1M F_{Chl} estimates and extracted Chl from water samples (Fig. 6). The percent difference between F_{Chl} using the median calibration slope and extracted Chl was ~60%, and values of 30% were typical. Correcting for temperature and CDOM fluorescence improved the relationship overall, however, only when a pigment specific calibration was applied to the CDOM- and temperature-corrected fluorescence (470 nm excitation), did the percent differences between estimated and measured decrease to < 30% for all observation and were typically valued at ~6% (Fig. 7).

Discussion

The detection of phytoplankton biomass via in situ Chl fluorescence observations is subject to variations induced by sensor design, phytoplankton concentration, composition and physiology, and environmental conditions. The interpretation of the fluorescence signal, because it is a relative measurement and does not have geophysical units in the absence of calibration, directly depends upon the magnitude of variations in fluorescence per Chl yield, which are, in turn, impacted by phytoplankton concentration, composition, and physiology induced by environmental conditions. So in many aspects, the factors impacting the detection of Chl fluorescence and

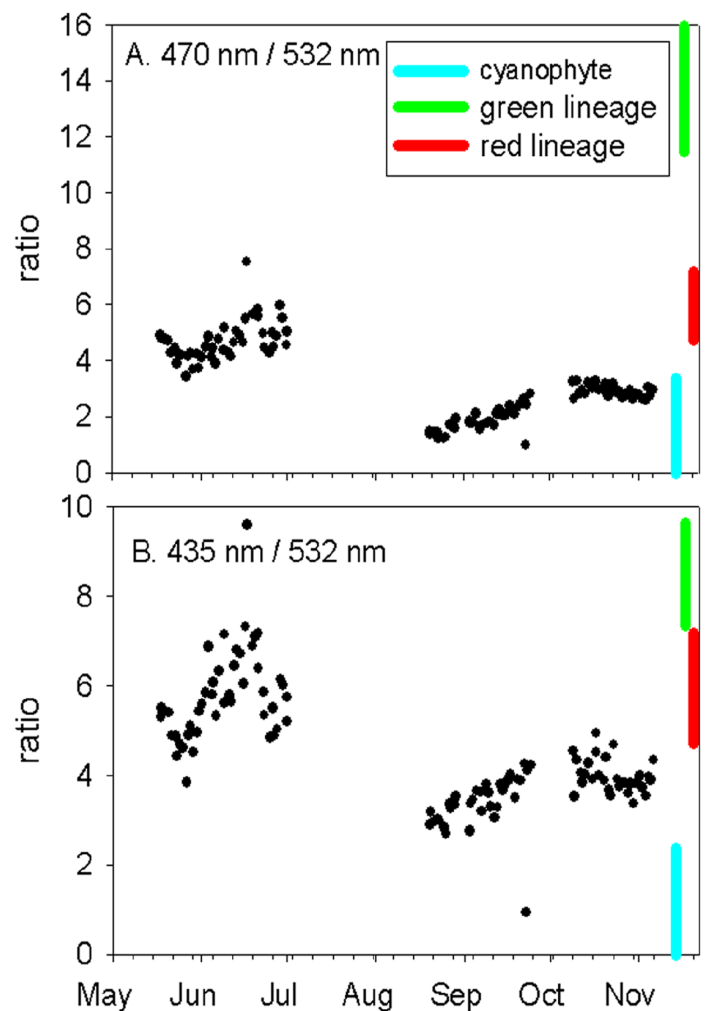


Fig. 5. Daily observations of fluorescence ratios measured with the 3X1M in China Lake, Maine, USA in 2006 and 2007. A. 470 nm/532 nm, B. 435 nm/532 nm. Vertical colored bars show the range in ratios for each pigment lineage. Data from May through July were collected in 2007, but are shown prior to the 2006 data to represent a typical continuous growth season. Ratios were corrected for DC_{dark} as well as temperature and CDOM fluorescence.

the factors impacting the interpretation of Chl fluorescence are the same. In this article, we investigated the factors impacting the detection of Chl fluorescence to provide some quantification on the sources of variability and on the confidence for in situ deployment of Chl fluorometers, and with

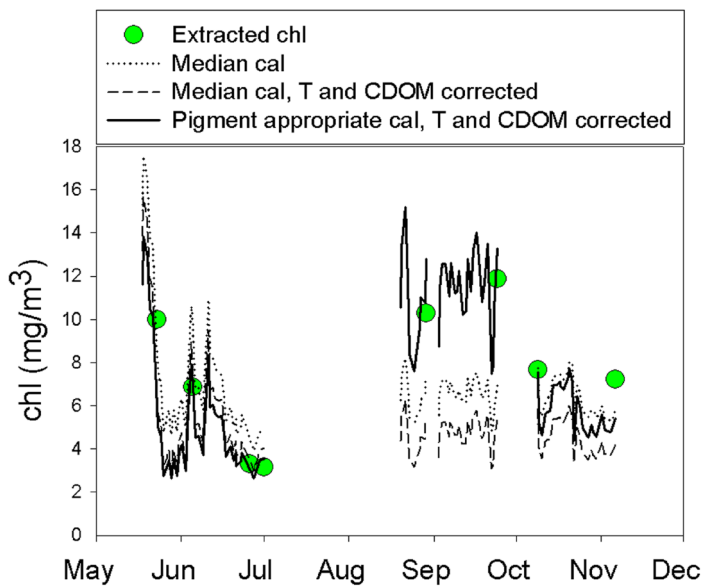


Fig. 6. Estimated Chl concentration time series for China Lake, Maine, over a growth season computed from observation of Chl *a* fluorescence from 440 nm excitation fluorescence using the median calibration slope (dotted), median calibration corrected for temperature and CDOM (dashed), and the pigment appropriate calibration slope, corrected for temperature and CDOM (solid). Extracted Chl concentration obtained from water samples indicated by symbols.

the goal to provide insight for the interpretation of the in situ Chl fluorescence as a proxy for phytoplankton biomass.

Sensor variability—Assessing the behavior of the instrumental dark current, DC_{dark} , is critical for tracking instrument drift and for quantifying both the instrumental noise and the signal to noise ratio, all of which need to be corrected (e.g., Roesler and Boss 2008). For tracking drift, we found the best choice was untaped measurements made in air (in a dark room with no reflections.) Air values reliably yielded consistent median values, and it was unnecessary to use tape because there were negligible differences between taped and untaped air values. Submerged in water, carefully taped sensors yield consistent and low values, however using tape poses several risks. If light leaks around or through the tape then the measurements will be too high. Also, applying tape can be messy and occasionally leaves residue on the sensor face. While water sources can be dirty or have differences due to scattering depending on the container they are measured in, optical measurements made in air are minimally affected by scattering and have much less variability.

Untaped readings made in optically pure water have a separate purpose. They are used to assess impacts of biofouling that can occur on even short deployments. Taking a post-recovery reading immediately following retrieval and then after cleaning provides the biofouling signal, which can then be used to post-correct deployment observations (Roesler and Boss 2008). We have found, however, that measurements

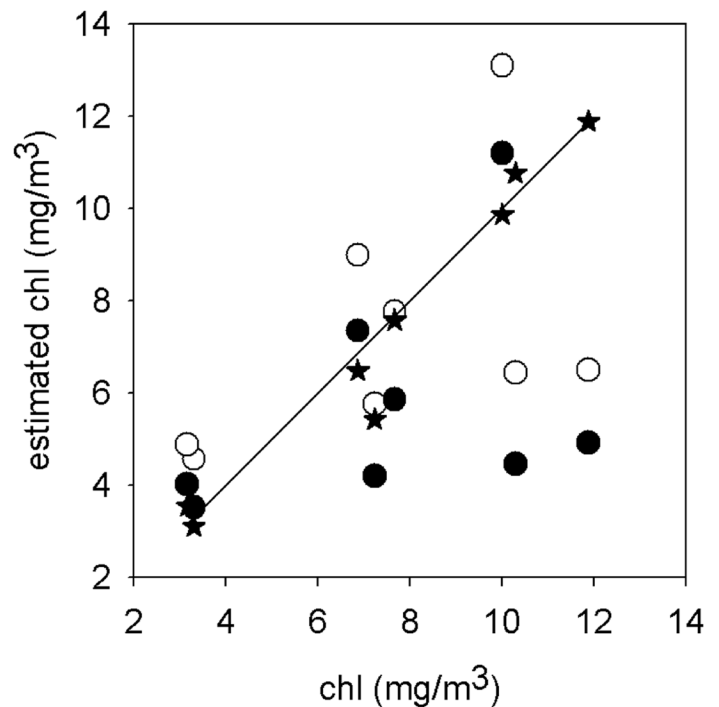


Fig. 7. Point-by-point comparison between extracted Chl *a* concentration determined from discrete water samples versus Chl estimated from in situ fluorescence with 435 nm excitation using the three calibration protocols in Fig. 6: median calibration, median calibration with temperature and CDOM corrections, and the pigment appropriate calibration corrected for temperature and CDOM (open circles, filled circle, and stars, respectively). The r^2 value changes from 0.24, 0.16, and 0.96, respectively. The solid line represents the 1:1 line.

made in ultra-pure water can result in variability in the blank reading caused by electronic instability. We find a small amount of conductance in the water, even the amount found in clean tap water, solves this problem (McGrath and Roesler unpubl. data).

Calibration regression offset—The calibration slopes calculated through regression can be applied to any environment as these characterize the quantitative sensor response; however the calculated intercept is influenced by the solution that was used in the dilution experiment. The regression intercept represents the fluorescence response of the particular experiment's diluent, which is not necessarily representative of field or even other lab conditions. Even clear-filtered seawater, freshwater, or culture media can contain CDOM or other materials that influence the measured blank reading and the calculated regression intercept. Consequently, the regression intercept should not be used as a DC_{dark} nor should a regression be calculated by correcting for blanks and forced through a zero intercept. Additionally, when performing standard curve dilution series for calibration, the diluent optical properties should be the same as those in the dissolved fraction of the starting culture. Otherwise, the fluorescence blank of each dilution will be different, and the resulting calibration slope will be biased.

Calibration suggestions—Due to CDOM and other sources of contamination, calibration dilution series should ideally be made with a filtrate that closely matches what the phytoplankton culture grew in, i.e., the culture filtrate. Additionally, the temperature of culture and the diluent should be the same (and measured directly in any case). These steps obviate the need to correct for differences in potential CDOM and temperatures responses between the culture filtrate and the diluent, for example, by using a BBFL2 CDOM sensor paired with your fluorometer. We found < 2% differences in slope between calibrations corrected and uncorrected for CDOM effects, however these differences could vary depending on the diluent that is used and the required sensitivity for low Chl conditions.

Pigment variability—In vivo fluorescence measurements of phytoplankton are affected by several sources of variability, including biomass concentration and differences in pigment composition between and within species (Sathyendranath et al. 1987). These sources of variability can be identified and quantified to improve estimates of biomass. The first source of variability is concentration. Phytoplankton photosynthetic pigments increase proportionately with biomass for a healthy culture in balanced growth, if all environmental factors are held constant (Cullen 1990). This relationship is one reason Chl *a* is a robust proxy for phytoplankton biomass. Under similar conditions, in vivo Chl fluorescence is linearly related to in vitro Chl concentration. Therefore the slope is defined by the ratio of the detected fluorescence response and Chl concentration with units (DC [mg Chl m⁻³]⁻¹) (Table 3). Such calibrations can be used to convert digital counts into Chl concentration estimates. Although extracted Chl concentration and fluorescence are conserved, once the pigment is packaged in a cell, the relationship is no longer conserved due to (1) packaging effects on the intracellular pigment concentration (Morel and Bricaud 1981; Kirk 1994), which “shade” pigment molecules from detection, thereby decreasing the apparent fluorescence efficiency of each Chl molecule; (2) pigment composition in which accessory pigments contribute to absorbed excitation energy, thereby increasing apparent Chl fluorescence efficiency (Poryvkina et al. 2000); (3) photochemical and non-photochemical quenching of fluorescence (Marra and Langdon 1993). These factors are impacted by phytoplankton composition and environmental acclimation as well as physiological response. Unsurprisingly, Chl concentration is predicted most accurately when the calibration regime that closely matches the measured phytoplankton is selected. Calibration slopes at all wavelengths can estimate biomass with approximately 5% to 10% error if the matching calibration is selected.

A useful aspect of fluorometers is that they measure in vivo fluorescence, which is often a more accurate representation of the effective Chl concentration (and therefore cell carbon biomass) than chemically measured in vitro Chl (“extracted Chl”). Phytoplankton pigment packaging sometimes causes in

vitro Chl and in vivo Chl fluorescence measurements of the same sample to yield different biomass estimates. Ratios of extracted-Chl to in vivo-fluorometrically-measured-Chl can vary by up to 10 times over small spatial and temporal scales. A large part of this variability occurs because phytoplankton are able to adjust their pigments on time scales of minutes to days (Cullen and Lewis 1988). Phytoplankton photoadapt to low light levels by producing more Chl and accessory pigments, while decreasing pigments in higher light. While these changes negligibly affect cell biomass, recall that Chl is used as a proxy for biomass. Consequently, these types of pigmentation changes alter the Chl-biomass ratio and affect the accuracy of biomass calculations. As the amount of Chl increases per cell, the fluorescence yield per Chl *a* decreases as chloroplasts become less efficient. Because these changes in Chl are inversely related to fluorescence yield, the ratio of biomass to calibrated in vivo Chl varies much less than the ratio of biomass to in vitro Chl. Thus, in situ estimates of biomass based upon fluorescence will necessarily be less variable. So whereas in vivo fluorescence measurements do not always match extracted Chl values, they are more representative of biomass, particularly when spatial and temporal patterns and gradients are examined.

For each species/growth condition, there was a specific calibration slope for each of the excitation channels because of the unique Chl *a* to accessory pigment ratio (generally corresponding to the 435 nm/470 nm or 435 nm/532 nm ratios). In theory, any of the three calibrated channels can be used to calculate Chl concentration; however the 435 nm channel corresponds to the Chl *a* absorption peak and had the smallest relative range in slope, followed closely by the 470 nm channel. The “all cultures” slope listed was the best first-order estimate of the Chl concentration for waters of unknown phytoplankton composition. Fluorescence ratios between the 3X1M excitation channels can be used to estimate pigment ratios, and hence phytoplankton composition, thereby allowing us to select a more specific calibration. This selection is accomplished by comparing the fluorescence ratios from a sample to the average determined for each pigment lineage (Table 4); this approach is most effective when a particular pigment group is dominant. However, the “all cultures” is still a good first-order estimate and can typically estimate biomass within a factor of 2. It is noteworthy that the diatoms used in this experiment have calibration slopes very close to the median slope of all cultures and to the median of the red lineage. What this suggests is that using one of the diatoms for a calibration standard curve will yield a robust slope for general purposes. This is particularly true for single excitation fluorometers.

The second order of variability is due to differences in pigment composition between species. All phytoplankton contain Chl *a*, however accessory pigments (e.g., Chls *b* and *c*, carotenoids and phycobilipigments) vary dramatically with taxonomy (e.g., Sathyendranath et al. 1987). Because Chl *a*

and each accessory pigment contribute differently to each excitation channel wavelength, each species has a unique slope for each channel. Similarities in pigmentation of species belonging to the same algal classes allow their slopes to be grouped together. Chlorophytes had the greatest median slopes at the 435 nm excitation channel due to their relatively high intracellular concentration of Chl *a*, but the smallest slopes at 532 nm because they have no accessory pigments at that wavelength. Cyanobacteria had high slopes at 532 nm because their phycobilipigments have peak absorption closest to that excitation channel. Optically, the phycobilipigment-containing classes of the red lineage (e.g., Cryptophyceae, Fig. 3) group better with the Cyanophyte pigment group than other phytoplankton in their lineage.

The magnitude of light absorption by photosynthetic pigments is the source of energy for Chl *a* fluorescence. Thus the differences in Chl *a* fluorescence response at the three excitation wavelengths provides a quantitative estimate of the relative photosynthetic absorption at those wavelengths (because each is essentially scaled to the same Chl *a* concentration and thus between species they are comparable too). Spectral similarities between groups are easily visualized in Fig. 1A and give a preview of the range in response slopes (Fig. 2) whereas Fig. 1B shows the spectral variations that were used as the basis for species discrimination. The 532 nm channel exhibits the most variability in pigment absorption, so it is not surprising that the ratios including it are most sensitive to species.

In total, approximately 71% of the percent difference between slopes was explained by species (pigment composition) differences, 17% by growth phase, and 12% by relative intracellular pigment concentrations (growth irradiance). The variance attributed to irradiance and growth phase was less than the 95% confidence intervals, except with particular species where there were large pigment differences with irradiance: *A. carterae*, *A. falcatus*, and *Anabaena* sp. Differences in pigmentation between species had a much larger impact on fluorescence than did irradiance. Whereas differences in slope between different types of phytoplankton were discernable, for most species differences due to irradiance were not. Variations in slope as a function of growth phase was not discernable except when the extremes (lag and log phases) in unbalanced growth conditions were included and broad 95% confidence limits on slope were observed.

Fluorometers come with a variety of excitation and emission wavelengths. Most fluorometers are standard equipped with a 470 nm LED, and some with lamp/filter combinations that yield an excitation peak at 440 nm. The trend is toward low power, small size, and high energy LEDs, and because of industry standards, the 470 nm channel is generally preferred. Even though 470 nm is not strictly the peak Chl *a* absorption wavelength, the energy transfer between the pigments absorbing at 470 nm and Chl *a* fluorescence is robust enough that this channel can be used effectively in lieu of a channel at the Soret peak. This channel shift does, however, necessitate cali-

bration with living cultures, because extracted Chl does not absorb at 470 nm.

We observed different calibration slopes for these two channels due to differences in sensor gain settings and due to differences in phytoplankton absorption and fluorescence quantum yield. However, the pattern in the calibration slopes between the two channels as a function of species is similar (Fig. 2), yielding a relatively invariant ratio (Table 4, Fig. 1C). Although the work presented in this paper is specific to the LED-type of sensor, the principles discussed here apply to all types of sensors.

Having a fluorometer with three wavelengths (such as the 3X1M) is valuable because it provides information about phytoplankton community composition, but also improves Chl concentration estimates because the calibration can be tailored to the species composition. Whereas both growth phase and growth irradiance impart statistically significant impacts on fluorescence yield, pigmentation differences between species were responsible for greater variations in fluorescence yield (Fig. 1C). Without information on ratios or some other way of discerning species, one is limited to using a single calibration (i.e., if you simply have a single excitation fluorometer). Selecting an appropriate calibration based on ratio estimates of pigment-based taxonomic composition greatly improves biomass estimates (Fig. 6 and Fig. 7).

Environmental variability—Phytoplankton biomass estimates from in situ fluorescence were greatly improved when corrected for temperature and CDOM fluorescence, with a pigment-specific calibration applied to best match the pigment ratios. While Chl estimates over this time period using only a single-excitation fluorometer are within a factor of 2-3 of extracted Chl measurements, our multi excitation fluorometer was able to resolve community composition on time scales of days and weeks. The ratios from in situ measurements in China Lake from May to June 2007 suggest a community of red lineage phytoplankton; cyanobacteria dominated in the late fall and transitioned toward a mixture of cyanobacteria and red lineage phytoplankton in mid-October 2006. This species succession matches the pattern of spring dominance by Bacillariophyceae followed by Cyanophyceae dominance observed since 1995 by the Kennebec Water District's microscope observations using a Sedgwick Rafter (Kennebec Water District 2005). By using our estimates of phytoplankton composition to apply pigment specific calibrations, biomass estimates were accurate within approximately 10%.

In conclusion, it is important to correct for the effects of temperature and CDOM on fluorometers, especially if they will be used for in situ measurements. Corrections vary with each sensor and each channel on each sensor, so it is important to perform sensor-specific calibrations after receiving them from the manufacturer, even if they are shipped with calibration corrections. To correct for temperature, fluorometers should be paired with a thermistor and a temperature calibration should be performed before deployments. To correct for CDOM, a fluorome-

Table 6. Sequence of equations to compute Chlorophyll *a* concentration from in situ Chl *a* fluorescence observations at three excitation wavelengths. The species-specific calibration slope, Slope_{ratio}, the temperature coefficient, $\Delta DC / \Delta T$, and the CDOM calibration slope, $CDOM_{cal}$, are determined experimentally in the laboratory.

Chl	$= CorrDC_{sample} \times (Slope_{ratio})^{-1}$	(3)
$CorrDC_{sample}$	$= DC_{sample} - DC_{dark} - DC_{CDOM}$	(4)
DC_{dark}	$= DC_{dark}(T_{cal}^0) + (T_{cal}^C - T_{insitu}) \times (\Delta DC / \Delta T)$	(5)
DC_{CDOM}	$= (CDOM_{DC insitu} - CDOM_{DC dark}) \times CDOM_{cal}$	(6)

ter measuring CDOM should be paired with the Chl fluorometer. The final equation for determining Chl is shown by the sequence of equations in Table 6, where the sample digital counts at each channel are corrected for (1) the difference between the in situ and calibration temperatures times the temperature dependence established in the laboratory for that channel and (2) the digital counts associated with CDOM fluorescence determined with a CDOM fluorometer corrected for dark (and temperature if necessary) and the CDOM response slope established in the laboratory (Fig. 4). Finally, the fluorescence ratios are calculated from the corrected observations to determine the phytoplankton composition (Table 4) and the appropriate Slope_{ratio} value (Fig. 2). Finally, the $CorrDC_{sample}$ is divided by the ratio-dependent calibration slope that best matches the phytoplankton composition. Applying all of these corrections ensures that biomass is predicted as accurately as possible. Application of this approach is generalized for any multispectral Chl *a* fluorometer once the fluorescence response has been established using a diverse set of species/growth conditions. The critical steps are quantifying the fluorescence response (which is particularly sensor dependent), the variations in the Chl-specific fluorescence (which is large determined by natural variations), the temperature response (sensor-specific), and the response to CDOM fluorescence (sensor dependent but the impact will be environmentally determined). When using a series of sensor of the same model, the full set of species calibrations need only be performed on one sensor to determine the response and natural variations; this sensor then becomes the “gold standard” against which additional sensors can be co-calibrated using a single species to determine instrument-specific response. A transfer function from this one species can be used to compute the fluorescence responses for the complete set, thereby obtaining an instrument-specific table of slopes and ratios akin to those found in Fig. 2.

References

Andersen, R. A. 2005. Algal culturing techniques. Elsevier/Academic Press. Belzile, C., C. S. Roesler, J. P. Christensen, N. Shakhova, and I. Semiletov. 2006. Fluorescence measured using the WETStar DOM fluorometer as a proxy for dissolved matter absorption. *Estuar. Coast. Shelf Sci.* 67:441-449 [doi:10.1016/j.ecss.2005.11.032].

- Bricaud, A., A. Morel, and L. Prieur. 1986. Absorption by dissolved organic matter in the sea (yellow substance) in the UV and visible domains. *Limnol. Oceanogr.* 26:43-53 [doi:10.4319/lo.1981.26.1.0043].
- Coble, P. G. 2007. Marine optical biogeochemistry: The chemistry of ocean color. *Chem. Rev.* 107(2):402-418 [doi:10.1021/cr050350].
- Cullen, J. J. 1982. The deep Chlorophyll maximum: Comparing vertical profiles of Chlorophyll. *Can. J. Fish. Aquat. Res.* 39:791-803 [doi:10.1139/f82-108].
- . 1990. On models of growth and photosynthesis in phytoplankton. *Deep Sea Res.* 37:667-683 [doi:10.1016/0198-0149(90)90097-F].
- , and M. R. Lewis. 1988. The kinetics of algal photoadaptation in the context of vertical mixing. *J. Plankton Res.* 10:1039-1063 [doi:10.1093/plankt/10.5.1039].
- , and R. F. Davis. 2003. The blank can make a big difference in oceanographic measurements. *Limnol. Oceanogr. Bull.* 12(2):29-35.
- Dickey, T. 1991. The emergence of concurrent high-resolution physical and bio-optical measurements in the upper ocean. *Rev. Geophys.* 29:383-413 [doi:10.1029/91RG00578].
- Falkowski, P. G., M. E. Katz, A. H. Knoll, A. Quigg, J. A. Raven, O. Schofield, and F. J. R. Taylor. 2004. The evolution of modern eukaryotic phytoplankton. *Science* 305(5682):354-360. [doi: 10.1126/science.1095964].
- , and J. A. Raven. 2007. Aquatic photosynthesis. Princeton Univ. Press.
- Holm-Hansen, O., C. J. Lorenzen, R. W. Holmes, and J. D. Strickland. 1965. Fluorometric determination of Chlorophyll. *J. Cons. Cons. Int. Explor. Mer* 30:3-15.
- Kennebec Water District. 2005. China water quality, algae blooms. Kennebec Water District.
- Kirk, J. T. O. 1994. Light and photosynthesis in aquatic ecosystems. Cambridge Univ. Press [doi:10.1017/CBO9780511623370].
- Kishino, M., M. Takahashi, N. Okami, and S. Ichimura. 1985. Estimation of the spectral absorption coefficients of phytoplankton in the sea. *Bull. Mar. Sci.* 37:634-642.
- Lorenzen, C. J. 1966. A method for the continuous measurement of the in vivo Chlorophyll concentration. *Deep-Sea Res.* 13:223-227.
- Lutz, V. A., S. Sathyendranath, E. J. H. Head, and W. K. W. Li. 2001. Changes in *in vivo* absorption and fluorescence spectra with growth irradiance in three species of phytoplankton. *J. Plankton Res.* 23:555-569 [doi:10.1093/plankt/23.6.555].
- Marra, J. 1997. Analysis of diel variability in Chlorophyll fluorescence. *J. Mar. Res.* 55:767-784 [doi:10.1357/0022240973224274].
- , and C. Langdon. 1993. An evaluation of an *in situ* fluorometer for the estimation of Chlorophyll *a*. Tech. Rep. LDEO-93-1. Lamont-Doherty Earth Observatory, Palisades, NY.

- Mitchell, B. G. 1990. Algorithms for determining the absorption coefficient of aquatic particulates using the quantitative filter technique (QFT), pp. 137-148. *In* Ocean Optics 10, Proc. International Society for Optical Engineering 1302.
- Morel, A. 1974. Optical properties of pure water and pure seawater. pp. 1-24. *In* N. G. Jerlov and E. Steeman-Nielsen (eds.), Optical aspects of oceanography. Academic.
- , and A. Bricaud. 1981. Theoretical results concerning light absorption in a discrete medium and application to specific absorption of phytoplankton. *Deep-Sea Res.* 28:1375-1393 [doi:10.1016/0198-0149(81)90039-X].
- Neale, P. J., J. J. Cullen, and C. M. Yentsch. 1989. Bio-optical inferences from Chlorophyll a fluorescence: What kind of fluorescence is measured in a flow cytometer? *Limnol. Oceanogr.* 34:1739:1748 [doi:10.4319/lo.1989.34.8.1739].
- Pegau, W. S., D. Gray, and J. R. V. Zaneveld. 1997. Absorption of visible and near-infrared light in water: the dependence on temperature and salinity. *Appl. Optics* 36:6035-6046 [doi:10.1364/AO.36.006035].
- Poryvkina, L., S. Babichenko, and A. Leeben. 2000. Analysis of phytoplankton pigments by excitation spectra of fluorescence, pp. 224-232. *In* EARSeL-SIG-Workshop LIDAR. Institute of Ecology/LDI, Tallinn, Estonia.
- Roesler, C. S. 1998. Theoretical and experimental approaches to improve the accuracy of particulate absorption coefficients from the Quantitative Filter Technique. *Limnol. Oceanogr.* 43:1649-1660 [doi:10.4319/lo.1998.43.7.1649].
- , and E. Boss. 2008. In situ measurement of the inherent optical properties (IOPs) and potential for harmful algal bloom (HAB) detection and coastal ecosystem observations, Chapter 5, pp. 153-206. *In* M. Babin, C. S. Roesler, and J. Cullen [eds.], Real-time coastal observing systems for marine ecosystem dynamics and harmful algal blooms: theory, instrumentation and modeling. UNESCO.
- , M. J. Perry, and K. L. Carder. 1989. Modeling in situ phytoplankton absorption from total absorption spectra. *Limnol. Oceanogr.* 34:1512-1525 [doi:10.4319/lo.1989.34.8.1510].
- , A. H. Barnard, G. Aiken, T. Huntington, W. B. Balch, and H. Xue. 2006. Using optical proxies for biogeochemical properties to study land coverage and terrestrial inputs of organic carbon into coastal waters from the Penobscot Watershed to the Gulf of Maine, pp. 9-13. *In* Proceeding of Ocean Optics XVIII, October, Montreal.
- Sathyendranath, S., L. Lazzara, and L. Prieur. 1987. Variations in the spectral values of specific absorption of phytoplankton. *Limnol. Oceanogr.* 32(2):403-415 [doi:10.4319/lo.1987.32.2.0403].
- Strickland, J. D. H., and T. R. Parsons. 1968. A practical handbook of seawater analysis. Pigment analysis. Bull. Fish. Res. Bd. Canada, 167.
- UNESCO. 1966. Determinations of photosynthetic pigments in seawater, Rep. SCOR/UNESCO WG 17, UNESCO Monogr. Oceanogr. Methodol., 1, Paris.
- University of Maine. PEARL. <http://pearl.maine.edu/>.
- Yentsch, C. S., and D. W. Menzel. 1963. A method for the determination of phytoplankton Chlorophyll and pheophytin by fluorescence. *Deep-Sea Res.* 10:221-231.

Submitted 2 February 2010

Revised 17 September 2010

Accepted 27 October 2010